THE
PHYSICAL REVIEW

A journal of experimental and theoretical physics established by E. L. Nichols in 1893

SECOND SERIES, VOL. 185, NO. 2 10 SEPTEMBER 1969

Crystal-Field Effects in Solid Solutions of Rare Earths in Noble Metals

GWYN WILLIAMS* AND L. L. HIRST†
Physics Department, Imperial College, London, S.W. 7, England
(Received 13 December 1968)

The magnetic susceptibility of some dilute alloys has been measured between 1.9 and 300°K by a force method. The investigation has been concerned mainly with solid solutions of 1 at. % or less of the elements of the second half of the rare-earth series in silver or gold, in order to study local moments of the impurity ions. The observed departures of the susceptibility from a Curie-Weiss behavior can be understood and fitted primarily in terms of crystal-field effects; the possible origins of such fields are discussed. It is found that the fitted crystalline fields are incompatible with a point-charge model, but can be explained by the hypothesis of a nonmagnetic 5*d* virtual bound state on the rare-earth impurity.

INTRODUCTION

CRYSTALLINE fields in rare-earth metals and alloys are of immediate importance to the understanding of such phenomena as magnetic anisotropy, magnetic symmetry structures, magnetostriction, and magnetic resonance. Comparatively few attempts have been made, however, to directly determine the crystalline-field parameters in metals as contrasted to insulators, and with the exception of the V_2 terms, even the order of magnitude and physical origin of the contributions are uncertain. A principal reason for the lack of experimental numbers is that in the pure rare-earth metals the crystalline-field splittings are generally smaller than the exchange coupling, so that a simple single-moment analysis is impossible.

In the present paper we report measurement and fitting of the magnetic susceptibilities of dilute alloys of heavy rare earths in Ag and Au.[1] These systems are in several respects more favorable than pure rare-earth metals for the determination of crystalline fields: (a) They are sufficiently dilute that interaction effects between moments are negligible at all but the lowest temperatures; (b) they have cubic symmetry, so that only the more interesting V_4 and V_6 components of the potential are involved; and (c) the electronic structure of the host is simpler, allowing perhaps more hope of an eventual understanding of the origins of the various terms.

METHODS AND MATERIALS

Measurements of the magnetic susceptibility χ between 1.9°K and room temperature were carried out on 2.5-mm-diam cylinders, 1–4 mm long (20–100 mg), using a sensitive null reading magnetic balance.[2] Measurements at room temperature 77, 4.2, and 1.9°K were carried out at eight different magnetic-field values, but at intermediate temperatures measurements were taken at a single-fixed-field value only.

Table I lists the alloys examined, indicates their source, and, in addition, indicates whether or not the alloy was subjected to metallographic analysis.[3] This table also includes an estimate of the effective moment per impurity atom, derived from the high-temperature (100–300°K) slope of the $1/\chi$ versus T plot, assuming the concentrations in the arc-melted and annealed samples to correspond to the weights of the starting materials.

Errors arising from drifts in the balance zero position, at intermediate temperatures, lead to an uncertainty of up to ± 0.015 dyn in the measured force on the sample. Since a temperature sensor attached directly to the sample would have drastically reduced the

* Present address: School of Mathematical and Physical Sciences, University of Sussex, Sussex, England.
† Now at Physik Department der Technischen Hochschule, Munich, West Germany.
[1] Preliminary report has been given by L. L. Hirst, Gwyn Williams, D. Griffiths, and B. R. Coles, J. Appl. Phys. **39**, 844 (1968). (The values given for $J_{s\text{-}f}$ in this paper should be corrected to 0.11 and 0.22 eV for *Ag* Er and *Au* Yb, respectively.)
[2] D. Griffiths, J. Sci. Instr. **38**, 463 (1961).
[3] P. E. Rider, K. A. Gschneider, and O. D. McMasters, Trans. AIME **233**, 1488 (1965).

TABLE I. Characteristics of the samples used.

Alloy	Nominal concentration of rare-earth (at.%)	Analyzed metallographically	Effective moment (in Bohr magnetons)	Theoretical moment (in Bohr magnetons)	Source
	0.8 Gd	Yes	8.0		a
Ag Gd	0.45 Gd	Yes	7.6	7.94	a
	0.1 Gd	Yes	8.0		a
Ag_3 Gd					b
Ag Tb	0.55 Tb	Yes	9.5	9.7	c
Ag Dy	0.86 Dy	Yes	10.8	10.6	a
	0.51 Dy	No[d]	10.9		a
Ag Ho	0.35 Ho	No[d]	10.2	10.6	a
	0.25 Ho	Yes	10.3		c
Ag Er	0.28 Er	Yes	9.8	9.6	c
	1.1 Er	Yes	9.8		c
Ag Tm	0.5 Tm	Yes	7.6	7.6	c
Ag Yb	0.5 Yb	Yes	Diamagnetic	4.5	c
Au Er	1.0 Er	No[e]	9.2	9.6	b
Au Tm	0.3 Tm	No[e]	7.7	7.6	f
Au Yb	0.9 Yb	No[e]	4.3	4.5	

[a] J. Bijvoet, Amsterdam.
[b] R. Harris, Birmingham.
[c] Johnson Matthey and Co., London.
[d] Insufficient material provided for analysis.
[e] None of the Au–rare-earth alloys were subjected to metallographic analysis since the rare-earth solubilities in Au are almost double those in the corresponding Ag alloy (see Ref. 3).
[f] A.E.R.E., Harwell.

balance sensitivity, the temperature of a copper cap surrounding the sample was measured. This arrangement leads to an error in temperature of ±0.5°K above 4.2°K and ±0.02°K below 4.2°K.

EXPERIMENTAL RESULTS

A. Non-*S*-State Impurities

The measured susceptibility versus temperature data points are given in Figs. 1–15 together with some theoretically fitted curves. The fits will be discussed later, but at this stage we wish to note the general features of the experimental results:

(a) At temperatures higher than about 100°K, the measured susceptibilities approach a Curie-law behavior, with an effective moment approximately that expected for the $4f$ electrons of an L-S coupled trivalent ion (Table I).

(b) At temperatures of a few tens of degrees, some but not all alloys show marked deviations from a Curie-

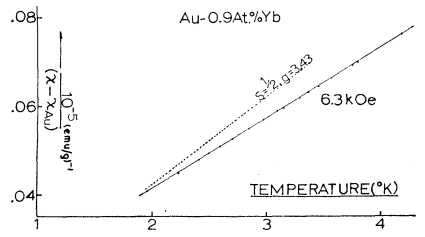

FIG. 2. Inverse susceptibility of Au-0.9 at.% Yb [(emu/g)$^{-1}$] in the liquid He temperature range.

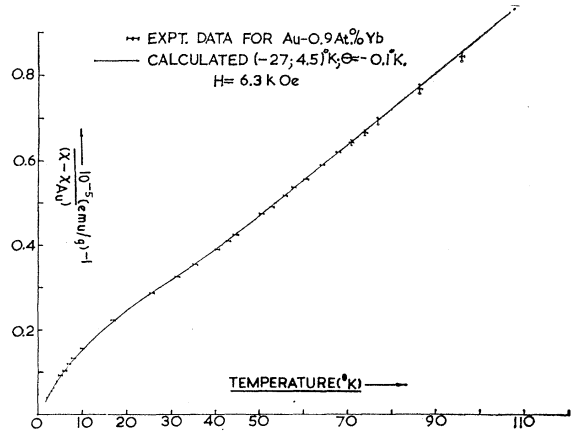

FIG. 1. Inverse susceptibility of Au-0.9 at.% Yb [(emu/g)$^{-1}$].

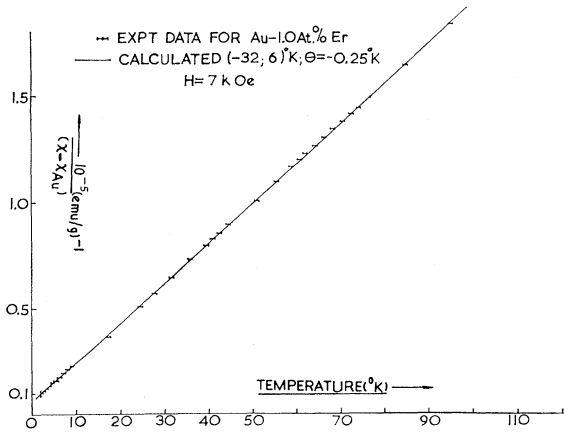

FIG. 3. Inverse susceptibility of Au-1.0 at.% Er [(emu/g)$^{-1}$].

law behavior. These effects are attributed to crystal-field splitting of the $4f$ core, as discussed in detail below.

Evidence of interaction effects is given by the M-H plots, some of which have been included. At the lowest temperature of 1.9°K these show considerable curvature; the curvature at high fields arises from Brillouin saturation but that at low fields can only arise from interactions. Such interactions are expected from indirect coupling via the conduction electrons, and

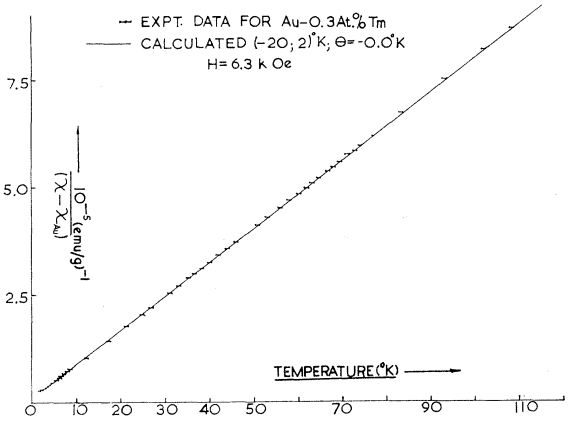

FIG. 4. Inverse susceptibility of Au-0.3 at.% Tm [(emu/g)$^{-1}$].

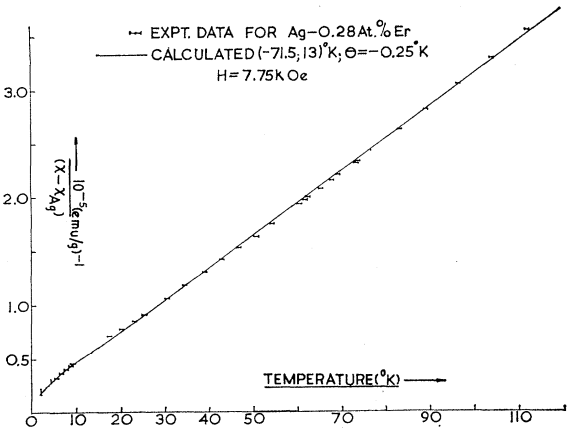

FIG. 5. Inverse susceptibility of Ag-0.28 Er [(emu/g)$^{-1}$].

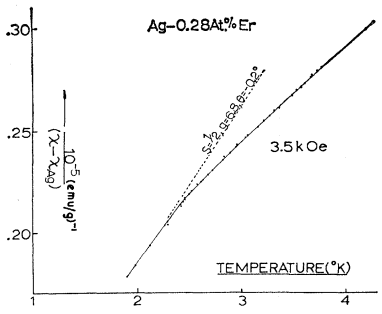

FIG. 6. Inverse susceptibility of Ag-0.28 at.% Er [(emu/g)$^{-1}$] in the liquid He temperature range.

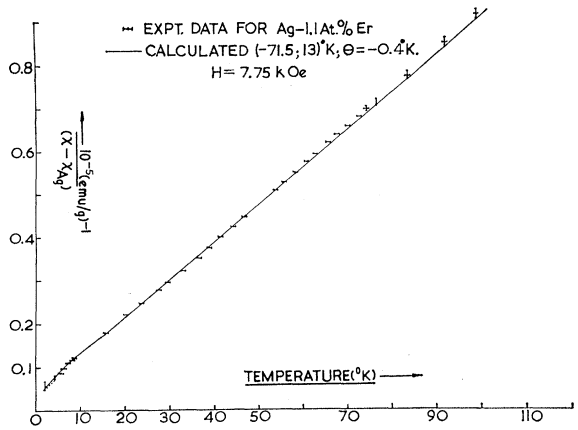

FIG. 7. Inverse susceptibility of Ag-1.1 at.% Er [(emu/g)$^{-1}$].

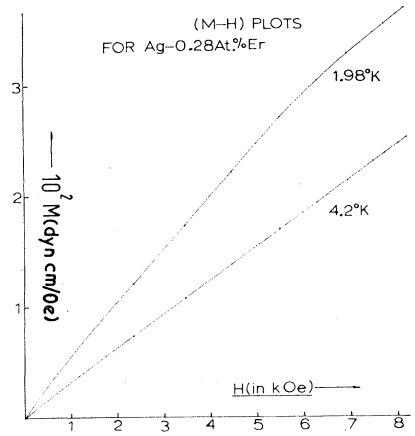

FIG. 8. Magnetization-field plots for Ag-0.28 at.% Er. [Throughout the magnetization is the specimen force (in dyn) divided by the field gradient (in Oe/cm).]

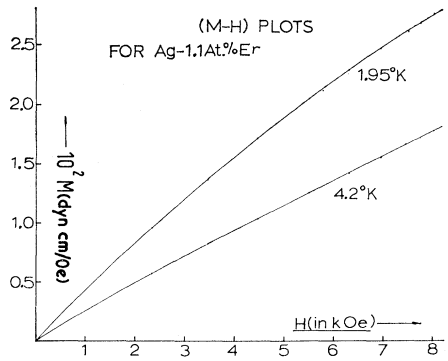

FIG. 9. Magnetization-field plots for Ag-1.1 at.% Er.

from magnetic-dipole coupling, the two contributions being roughly comparable. These interaction effects are of some interest in themselves. In pactice, however, it would be extremely difficult to make calculations of these effects which would be sufficiently accurate to aid in analysis, so we must simply regard these as

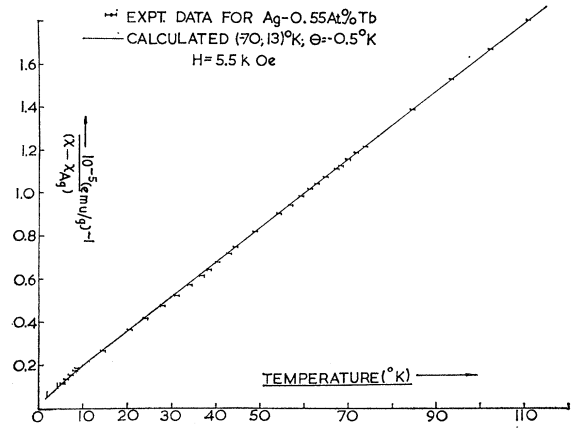

FIG. 10. Inverse susceptibility of Ag-0.55 at.% Tb [(emu/g)$^{-1}$].

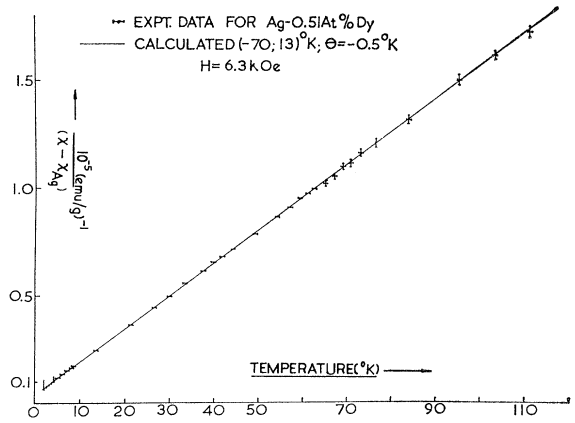

FIG. 11. Inverse susceptibility of Ag-0.51 at.% Dy [(emu/g)$^{-1}$].

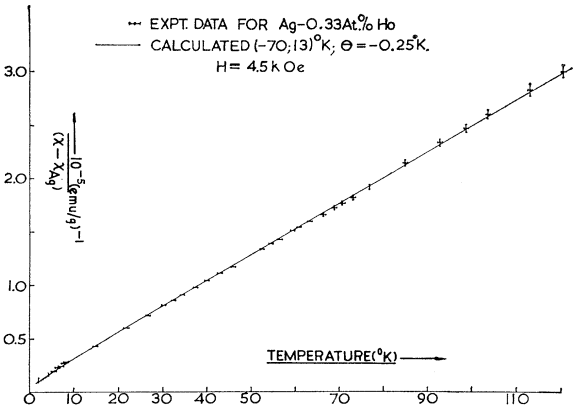

FIG. 12. Inverse susceptibility of Ag-0.33 at.% Ho [(emu/g)$^{-1}$].

"errors" from the point of view of the single-impurity theory. To arrive at a measure of this error, we compare M/H at the value H_0, which is our primary definition of the susceptibility, with the slope of the M-H plot as estimated in the region above the low-field curvature this can only be done, of course, at the "fixed" temperature). These two values of the susceptibility are regarded as determining an "error bar" in the low-temperature region, *where the true experimental errors (due to zero-field drifts, etc.) are quite negligible.* The experimental susceptibility error at higher temperatures, and the temperature error, both of which have been discussed previously, are also indicated in the data plots. These plots are given as inverse susceptibility against temperature, and in some cases have been fitted with the single-impurity theory (discussed in the next section) also allowing a small Θ. This amounts simply to a uniform "shift" along the temperature axis, and is a "first-order" attempt to account for interaction effects (Θ is never more than a fraction of a degree, and in all cases roughly consistent with the magnitude of internal fields, as estimated from the low-field M-H curvature).

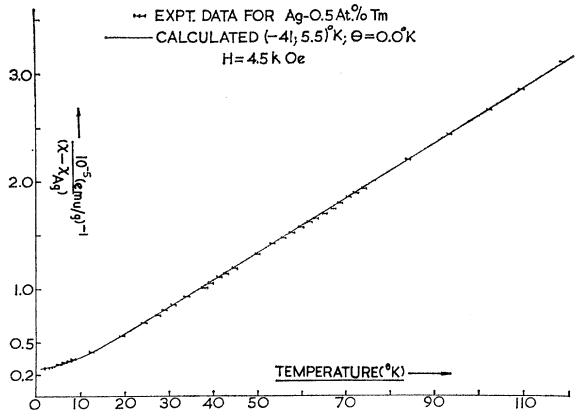

FIG. 13. Inverse susceptibility of Ag-0.5 at.% Tm [(emu/g)$^{-1}$].

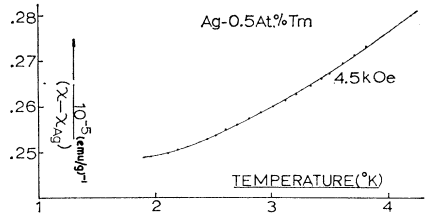

FIG. 14. Inverse susceptibility of Ag-0.5 at.% Tm [(emu/g)$^{-1}$] in the liquid He temperature range.

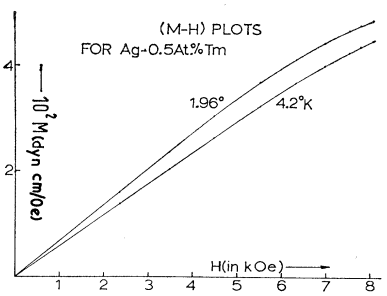

FIG. 15. Magnetization-field plots for Ag-0.5 at.% Tm.

B. S-State Impurities (Gd^{3+})

Since the orbital angular momentum of Gd^{3+} vanishes to lowest order, a crystal-field splitting of the order of only 1°K is expected, which should have no appreciable effect on the susceptibility in the temperature range measured here. Nevertheless, early measurements on Ag-0.5 and 0.8 at.% Gd alloys showed susceptibility behavior qualitatively similar to that attributed to crystal-field splitting in non-S-state alloys. Metallographic analysis revealed the presence of an intermetallic second-phase compound in these alloys (although x-ray measurements had failed to detect it). The Ag-Gd phase diagram[4] indicated that this second-phase compound was likely to be Ag_3Gd, whose typical antiferromagnetic susceptibility (Fig. 16) added to a Curie susceptibility for the primary phase, would account satisfactorily for the measured results. This experience emphasizes the necessity for great metallurgical care, and prompted us to make metallographic checks on most of our subsequent samples.

The Ag-0.1 at.% Gd alloy contained no second-phase compound; a Curie-Weiss temperature dependence of its magnetic susceptibility was observed (Fig. 17), from which "Θ"≈ -2°K. The M-H plots for this alloy are reproduced in Fig. 18, their nonlinear character being similar to that observed for CuMn.[5] Brillouin curvature accounts for the "high-field" ($H/T>2$ kOe/°K) nonlinearity, while the low-field curvature is indicative of interaction effects. If the latter are discussed in terms of an internal-field mechanism, the low-field curvature of the M-H plots indicate that the magnitude of such a field would be roughly 5 kOe at the lowest experimental temperature ($\mu H_{\text{int}} \approx 3$°K for $\mu = 8\mu_B$). The unexpectedly large experimental value for Θ necessitates some comment: In alloys containing

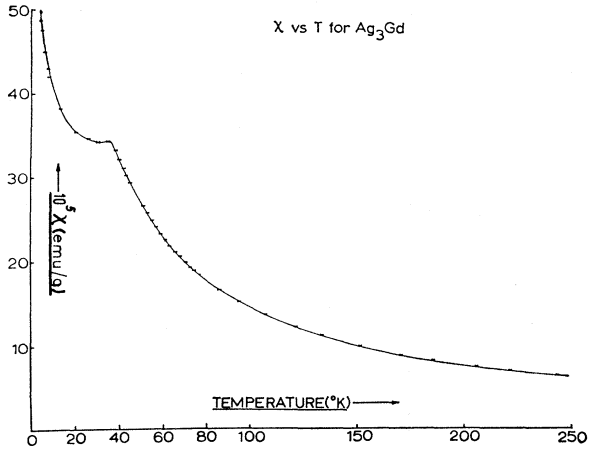

FIG. 16. Measured susceptibility of Ag_3Gd [(emu/g)].

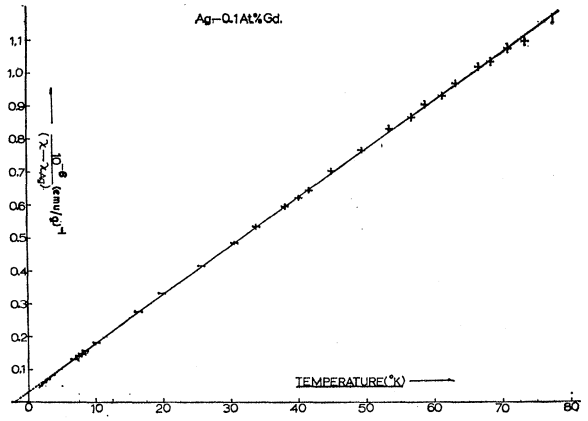

FIG. 17. Inverse susceptibility of Ag-0.1 at.% Gd [(emu/g)$^{-1}$].

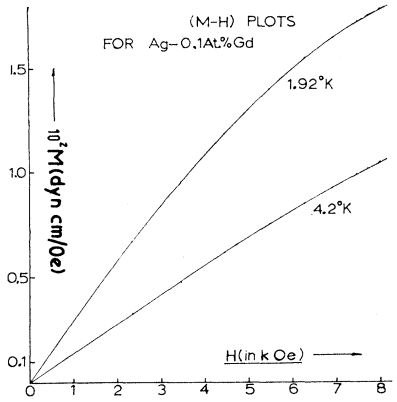

FIG. 18. Magnetization-field plots for Ag-0.1 at.% Gd.

small amounts (0.1 at.% or less) of Gd, the value of $(\chi-\chi_{\text{host}})^{-1}$, particularly above the liquid He region, is critically dependent on the value taken for the host susceptibility. In the present case the susceptibility of pure Ag, as reported in Ref. 6, has been used; however, it is clear that the addition of three electron per Gd atom to the conduction band of the host will modify its susceptibility. Consequently the value of χ_{host} used is that which should have been used in that of a Ag-0.1 at.% Lu alloy.

CRYSTAL-FIELD FITS TO THE SUSCEPTIBILITY DATA

The most general operator equivalent potential, with cubic point symmetry, within a manifold of total angular momentum $J\hbar$ composed of f-electron wave functions may be written in the form[7]:

$$H = C_4\beta(O_4^0 + 5O_4^4) + C_6\gamma(O_6^0 - 21O_6^4). \quad (1)$$

The O's are the operator equivalents and the β and γ multiplicative factors, both of which have been tabu-

[4] K. A. Gschneider, in *Rare Earth Alloys* (D. Van Nostrand Company, Inc., New York, 1961), p. 280.
[5] R. W. Schmitt and I. S. Jacobs, J. Phys. Chem. Solids 3, 324 (1957).
[6] C. M. Hurd, J. Phys. Chem. Solids 27, 1371 (1966).
[7] See, for example, J. M. Baker, B. Bleaney, and W. Hayes Proc. Roy. Soc. (London) A247, 141 (1958).

lated by Stevens.[8] The crystal-field parameters C_4 and C_6 are the coefficients of Y_4^0 and Y_6^0 in a spherical-harmonic expansion of the crystal potential, multiplied, respectively, by the expectation values $\langle r^4 \rangle$ and $\langle r^6 \rangle$ of the $4f$ wave functions. Since these expectation values are not expected to differ greatly among the heavier rare earths, at least for trivalent ions,[9] the crystal-field model in its most literal form (where the values of the field set up by the lattice are supposed to be independent of the probing ion) would imply that the values of C_4 and C_6 should be the same for different rare earths in a given matrix.

It is usual, however, to regard such coefficients as parameters to be determined from the experimental data. When trial values for C_4 and C_6 have been specified, it is possible to write explicitly the $(2J+1) \times (2J+1)$ crystal-field matrix for a given constant J manifold. We have written a computer program to diagonalize such matrices, and calculate, from the eigenvalues and eigenvector, the (temperature-dependent) magnetic susceptibility. The diagonalization is carried out including the Zeeman splitting in the finite experimental field, so that any Brillouin saturation effects are automatically included.

The theoretical susceptibility-temperature curves, from computations using a wide range of crystal-field parameters, are generally less dramatic than those familiar from cases of lower-than-cubic symmetry. In the cubic case, the introduction of crystalline-field effects must always reduce the susceptibility (raise the reciprocal susceptibility) as compared with the free ion Curie law, but the change is often quite small and is often apparent only at very low temperatures. As a general rule, striking deviations from a Curie law behavior are seen only at temperatures below one third of the ground-state isolation. This situation means that we cannot, as we would wish, fit both parameters for each alloy independently. Instead, effort must be focussed on those cases for which the susceptibility shows the most "character," or where some assistance comes from an EPR identification of the ground state, and then inquire whether the remaining cases are consistent with reasonable values of $(C_4; C_6)$. Although we do not expect the crystal-field model to hold in its most literal form, which would require the parameters to be strictly constant in a given matrix, we do require that they should not vary radically, that is, that they should retain the same signs and roughly the same magnitudes within each matrix.

In the cases where EPR has been seen,[1,10] it has been attributed to crystal-field ground states whose symmetry type occurs only once for the ion in question. Its state vector and the theoretical g value are thus independent of the crystal-field parameters, so that the experimental g value does not provide a determination but only sets certain limits on the ratio C_4/C_6 such that the state in question should lie lowest. Nevertheless it will be seen that the EPR evidence is very helpful in eliminating ambiguity from the fits; in addition, the close agreement of the experimentally measured g values with those given by the theory without any adjustable parameters gives one confidence that one is dealing with a genuine crystal-field problem, with a well-defined integar number of $4f$ electrons, L-S coupled to yield maximum J.

We now proceed to a discussion of the individual cases, the range of best fit parameters having been chosen such that the associated curves pass through the extremities of the "error bars" mentioned in the previous section.

Au Yb

The susceptibility-temperature data, reproduced in Fig. 1, deviates so markedly from Curie-Weiss form in this case that it alone suffices to determine both crystal-field coefficients:

$$C_4 = -27 \pm 3°\text{K}; \quad C_6 = 4.5 \pm 0.3°\text{K} \ (|\Theta| < 0.1°\text{K}).$$

These signs are consistent with the EPR identification[10] of the ground state as Γ_7 (Bethe's notation).[11]

Figure 2 is a detailed plot of the experimental low-temperature points.

Au Er

In this alloy, EPR measurements[10] indicate that Γ_7 is again the ground state, however, this observation merely requires C_6 to be positive. Assuming that the signs of the coefficients of the terms in the crystal-field Hamiltonian are the same for all rare earths in a given matrix implies that C_4 is negative. With this restriction the susceptibility-temperature data on this alloy (Fig. 3) yields the following limitation on C_4 and C_6:

$$C_4 = -32 \pm 4°\text{K}; \quad C_6 = 6.0 \pm 0.5°\text{K} \ (\Theta = 0 \text{ to } -0.5°\text{K}).$$

These values are roughly consistent with those deduced in the previous case.

Au Tm

For *Au* Tm (non-Kramer's) the only available information is the experimental susceptibility-temperature data. With the previous assumption about the signs of C_4 and C_6, fitting the experimental data yields the following results:

$$C_4 = -18.5 \pm 1.5°\text{K}; \quad C_6 = 2.0 \pm 0.1°\text{K} \ (\Theta = 0).$$

Clearly, the values deduced for the previous alloys lie well outside the error associated with fitting this data,

[8] K. H. W. Stevens, Proc. Phys. Soc. (London) **A65**, 209 (1952).
[9] A. J. Freeman and R. E. Watson, in *Magnetism*, edited by G. T. Rado and H. Suhl (Academic Press Inc., New York, 1965), Vol. IIA, p. 292.
[10] D. Griffiths and B. R. Coles, Phys. Rev. Letters **16**, 1093 (1966).
[11] K. R. Lea, M. J. M. Leask, and W. P. Wolff, J. Phys. Chem. Solids **23**, 1381 (1962).

and we are forced to conclude that the $(C_4; C_6)$ values are not constant for different rare earths in a given matrix.

In the case of the dilute Ag–rare-earth alloys, the EPR identification of the Γ_7 ground state in *Ag* Er implies that C_6 is positive, although both signs for C_4 are possible. Although a detailed discussion will not be given, the assumption that C_4 is positive throughout the Ag alloys would require a large variation in the magnitudes of the parameters from one alloy to another for a satisfactory fit to the susceptibilities. In what follows we therefore take C_4 and C_6 to be negative and positive, respectively.

Ag Er

Fits to the experimental data of Figs. 5 and 7 yield

Ag-0.28 at.% Er: $C_4=-70\pm2$°K; $C_6=13\pm0.2$°K ($\Theta=0$ to -0.3°K),

Ag-1.1 at.% Er: $C_4=-70\pm2$°K; $C_6=13\pm0.2$°K ($\Theta=0$ to -0.8°K).

These parameters correspond to an over-all splitting of about 210°K.

Ag Tb, *Ag* Dy, and *Ag* Ho

In all these alloys the deviations from a Curie law were too slight to yield unique determinations of the parameters. However, the data is consistent with the parameter values given above for *Ag* Er, these values having been used to obtain the theoretical curves of Figs. 10–12. Furthermore, parameters near these values yield a Γ_8 quartet ground state for *Ag* Dy. This seems to be required by the experimental absence of EPR in powder samples, since such resonances ought to appear with a Γ_6 or Γ_7 ground state (expected g values $=6.67$ and 7.55, respectively). The Γ_8 quartet does not have full rotational isotropy[12] and would be expected to give EPR only in a single-crystal specimen.

The $(-70; 13)$°K values for $(C_4; C_6)$ yield nonmagnetic Γ_3 ground states for *Ag*Ho and *Ag*Tb; their isolations from the next levels are, however, quite small (<1°K).

Ag Tm

Finally, we are left with the *Ag* Tm data (*Ag* Yb being unfortunately diamagnetic and Yb presumably divalent). The range of fits to the experimental data (Fig. 13) is

$$C_4=-30 \text{ to } -41\text{°K}; \quad C_6=5.4 \text{ to } 5.5\text{°K} \ (\Theta=0),$$

corresponding to well-isolated (approximately 20°K) Γ_2 singlet ground state. We note that in this case, and also to a lesser extent for *Au* Tm, the presence of an isolated nonmagnetic ground state is clear from the form of the inverse susceptibility versus temperature curves (Figs. 4 and 14), which tend to flatten out towards a finite low-temperature limit. This bears an interesting relation to the low-temperature M-H plots (Fig. 15), which, unlike those for previous alloys, show no low-field nonlinearity. This is precisely what is expected, since at sufficiently low temperatures only the nonmagnetic ground state is appreciably occupied and so both indirect interactions via the conduction electrons and dipole-dipole interactions must vanish. However, the "mixing" induced by the application of a magnetic field destroys the nonmagnetic character of such a ground state, and the associated effects of this can clearly be seen at higher fields.

In summary, we find that if we require the crystal-field parameters to be strictly constant for all impurities in a given matrix, a satisfactory fit is not possible; if we allow the parameters to vary arbitrarily from one impurity to another, a wide range of fits is possible in most cases. However, by requiring the parameters to have similar values within a given host, i.e., the same signs and similar magnitudes, we find that a satisfactory fit requires that C_4 be negative and C_6 positive for both Ag and Au materials. In addition, the magnitudes of these parameters (a) vary by almost a factor of two within both alloy series; (b) yield over-all splitting of the order of 100°K in Au-based alloys and 200°K in Ag-based alloys, and (c) when substituted into Eq. (1) indicate that in general the fourth-order terms are only marginally more important than the sixth-order terms in determining the over-all splitting.

ORIGINS OF THE CRYSTAL FIELD

The first possible source of crystal field which should be considered is the direct electrostatic effect of the lattice. Traditionally, one has proceeded by representing the lattice ions as point charges, and although this model is now regarded with some suspicion it does seem to account roughly for the lower-order crystal-field terms in the pure rare-earth metals.[13] The conduction electron charge density must also be considered since it will not be uniform, but will have a radial spatial dependence about the lattice-ion sites: In the ion interiors it will be reduced because of orthogonality requirements, while immediately outside them it will be increased by screening tendencies. To the extent that these conduction-electron charge density variations are purely radial, as would be expected on some of the simpler screening models, they can be considered simply to change the values of the effective lattice point charges.[14] The potential arising from point charges (of magnitude $Z|e|$, say) located at the fcc nearest-

[12] B. Bleaney, Proc. Phys. Soc. (London) **73**, 979 (1959).

[13] R. J. Elliott, in *Magnetism*, edited by G. T. Rado and H. Suhl (Academic Press Inc., New York, 1965), Vol. IIA, p. 385.

[14] Using a crude model of inpenetrable lattice ions surrounded by conduction electrons obeying the Thomas-Fermi equation, we estimate the net conduction electron effect as an enhancement of the effective ionic charge by $0.3|e|$, too small to be qualitatively important.

neighbor sites is found to be

$$C_4=\frac{7\sqrt{2}}{8}\frac{Ze^2}{a^5}\langle r^4\rangle_{4f},$$

$$C_6=\frac{39\sqrt{2}}{32}\frac{Ze^2}{a^7}\langle r^6\rangle_{4f}.$$

Using $a=4.1$ Å, the unit cell edge in Ag or Au, putting $Z=1$, and using the values $\langle r^4\rangle_{4f}\approx a_0^4$, $\langle r^6\rangle_{4f}\approx 4a_0^6$ (a_0 being the Bohr radius) calculated for three, trivalent rare-earth ions in the second half of the series by Freeman and Watson,[9] then

$$C_4\approx 14°\text{K} \quad \text{and} \quad C_6\approx 1.5°\text{K}.$$

These values are up to a factor of five too small as compared with our experimental fits. Rather more serious is the fact that the sign of the leading C_4 term (depending only on the symmetry of the model) is given incorrectly. Furthermore, it is difficult to see how any simple lattice-charge model can provide the observed factor of two variations of parameters within a given metallic matrix.

The occurrence of a $5d$ nonmagnetic virtual bound state (vbs) on the rare-earth impurity has been suggested[15] as a possible explanation for the observed crystal-field parameters. The arguments in favor of this proposition certainly appear convincing: The need to screen the excess charge on the (trivalent) rare-earth impurity is a prerequisite in a metallic host, while the screening electrons must be in states orthogonal to both the partly filled $4f$ and the closed shells. Spectroscopic data on the pure rare earths[16] (outer electron configuration $5d^16s^2$) certainly suggest that the lowest lying state satisfying the orthogonality criterion is the $5d$. With reference to the free atom configuration it may be argued from the "Friedel" point of view, that the loss of three valence electrons would result in an impurity potential capable of partially binding a screening electron in a broadened atomic state of d-like symmetry. The experimental evidence gathered on the first row ($3d$) transition metal impurities in noble metal hosts reinforces this point of view, and moreover indicates that the number of electrons accommodated in $3d$ virtual bound screening states is close to the number occupying these $3d$ states in the free atom. In addition the general trend towards nonmagnetic virtual states as one passes from 1st row to 3rd transition metal impurities in a given host, leads to the conclusion that the $5d$ vbs in question will be both nonmagnetic and occupied by only one electron. Experimentally, it is quite clear that in our case any $5d$ vbs must be unmagnetized, since the effective moment values and (a yet more sensitive test) the g values for EPR give no indication of an extra contribution.

The presence of such a state would give special properties to the surrounding charge cloud, consequently the preceding arguments must be reconsidered. Provided the width of this vbs is comparable with, or smaller than, the crystal-field splitting of the $5d$ orbitals, the vbs will have an aspherical (but cubic) charge distribution which will contribute to the effective crystalline-field experienced by the $4f$ electrons. The three so called $d\epsilon$ [17] (Γ_5) orbitals, having angular dependence xy, yz, and zx extend towards the positively charged nearest-neighbor sites in the fcc lattice, while the two $d\gamma(\Gamma_3)$ orbitals (having angular dependence x^2-y^2, $3z^2-r^2$) extend into regions "midway" between the fcc nearest neighbors. This geometry means that the $5d\epsilon$ orbitals will have lower energy than the $5d\gamma$ orbitals, and in addition the charge distribution associated with the former is such as to produce a negative contribution to the crystal-field parameter C_4 seen by the $4f$ core.

Let us consider some of the magnitudes involved. First of all, the appropriate radial integral from the $4f$-$5d$ Coulomb interaction, $F^4(4f,5d)$ in Slater's notation, is evaluated[18] as 8115 cm^{-1} using Hartree-Fock wave functions for $Eu^+(4f^75d^1)$. Because of the small $4f$-$5d$ overlap, the corresponding exchange terms are small in comparison. Inserting the appropriate angular integrals and conventional numerical factors, this interaction yields the crystalline-field parameter (from this source)

$$C_4=-113\ \text{cm}^{-1}\ (-158°\text{K}),$$

where we have assumed a net total of one $5d$ electron in a real bound state composed equally of the three $5d\epsilon$ orbitals. However, the contribution from a vbs will be reduced from this value, for two reasons: First, because the finite width of the vbs will cause some population of the $5d\gamma$-type orbitals, with consequent cancellation of the nonspherical part of the potential; and second, because the total $5d$ population will decrease from one toward zero as the $5d$ energy rises from below to above the conduction-electron Fermi energy.[19] We will not attempt to estimate the second effect since an *a priori* estimate of the $5d$ energy is so difficult. Concerning the first, the splitting of the $5d$ orbitals by the lattice charges should be roughly comparable with that of $3d$ orbitals in first-transition ions, i.e., $\sim$1 eV,[20] while the width of the vbs might be estimated at 1 eV also, implying a reduction of the effect to a

[15] B. R. Coles and R. Orbach (private communication).
[16] B. G. Wybourn, in *Spectroscopic Properties of Rare Earths* (Wiley-Interscience, Inc., New York, 1965), Chap. 1.
[17] This is the notation used, for example, by F. G. Von der Lage and H. Bethe, Phys. Rev. **71**, 612 (1947).
[18] We are grateful to J. V. Mallow and Professor A. J. Freeman for providing this value (private communication).
[19] The $5d$-$5d$ Coulomb repulsion will be strong enough to prevent a population of *more* than one $5d$ electron for any reasonable binding potential.
[20] See, for example, B. Bleaney and K. H. W. Stevens, Rept. Progr. Phys. **16**, 108 (1953).

TABLE II. Summary of the more important details of the experimental results.

Alloy	Typical parameters C_4(°K)	C_6(°K)	Ground state	Ground-state isolation (°K)	1st excited state	Over-all splitting (°K)
Ag Tb	−70	13	Γ_3	<1	$\Gamma_5^{(2)}$, Γ_2	117
Ag Dy	−70	13	Γ_7	1	$\Gamma_8^{(1)}$	157
Ag Ho	−70	13	$\Gamma_3^{(2)}$	<1	$\Gamma_4^{(2)}$	182
Ag Er	−70	13	Γ_7	35	$\Gamma_8^{(1)}$	207
Ag Tm	−30	5.5	Γ_2	22	$\Gamma_5^{(2)}$	97
	−41	5.5	Γ_2	20.5	$\Gamma_5^{(2)}$	118
Au Er	−33	6.5	Γ_7	19	$\Gamma_8^{(1)}$	105
Au Tm	−17	2	Γ_2	7	$\Gamma_5^{(2)}$	47
Au Yb	−27	4.5	Γ_7	79	Γ_8	83

fraction of the real bound-state value given above; however, the width of the vbs is again dependent on its energy.

In summary we propose that a nonmagnetic 5*d* vbs is split by the action of the lattice ions, and itself in turn provides the splitting of the 4*f* core which is directly observed in the magnetic properties. This contribution has the right sign and sufficient magnitude to account for the observed fourth-harmonic crystalline field. Further, it should be sensitive to changes in the energy of the vbs. The situation is thus to be contrasted with the case of rare earths in insulators, where electrons in shells other than the 4*f* are regarded as shielding the "magnetic" electrons from the electric field produced by the lattice charges[21] (although antishielding can occur), whereas in the present context the charge distribution associated with a screening electron in a 5*d* vbs is regarded as providing the dominant contribution to the fourth-order 4*f* crystal-field potential. On the other hand, to the extent that the 5*d* functions involved are true $l=2$ orbital eigenfunctions, no contribution to the sixth harmonic crystal field can arise. The observed magnitude of C_6 is thus unexplained since the point charge estimated lattice contribution is too small. Problems involving impurities in metals are extremely subtle and difficult, and it may be that the simple picture presented would not stand up under more thorough investigation; on the other hand, it might conceivably be found that higher-angular-momentum components in the screening cloud around the rare-earth ion would provide the needed sixth harmonic contribution. In any case, we believe the model merits a more ambitious theoretical investigation.

Table II summarizes the more important details of the experimental results (using typical best-fit crystal-field parameters).

[21] A. J. Freeman and R. E. Watson, Phys. Rev. **139**, A1606 (1965).

SUMMARY

We have found that the magnetic properties of dilute alloys of the heavy rare-earths in Ag or Au can be understood by assuming the rare-earth ions to be in well-defined (trivalent) charge states, with the magnetic 4*f* cores influenced by a crystalline field with the cubic symmetry of the host. The strength of this crystalline field causes an over-all splitting of typically 100°K in Au-based alloys, and 200°K in Ag-based alloys. Calculations based on a crystalline-field effective potential produced simply by effective point charges located on nearest-neighbor sites in the fcc host lattice yield the correct sign but insufficient magnitude for the "V_6 term." However, such a model accounts neither for the sign nor magnitude of the "V_4 term," nor does it yield the atomic number dependence of our best-fit parameters. The hypothesis of a nonmagnetic 5*d* vbs on the rare-earth impurity, on the other hand, with its associated effect on this "V_4 term," does appear capable of explaining the data.

ACKNOWLEDGMENT

We are indebted to Professor B. R. Coles for suggesting this problem, for continued discussion, and especially for suggesting (with Professor R. Orbach) the existence of a 5*d* vbs as a source of the crystalline fields. We would also like to thank Professor R. Orbach and Professor A. J. Freeman for several informative discussions. Dr. J. Bijvoet, Dr. R. Harris, Dr. J. Penfold (A.E.R.E., Harwell), and J. Day (Johnson Matthey and Co., London) are thanked for the provision of alloys. This research formed part of a program supported by the United Kingdom Atomic Energy Authority.